Minerals Engineering 160 (2021) 106680

Contents lists available at ScienceDirect

Minerals Engineering

journal homepage: www.elsevier.com/locate/mineng

Separation of particles of different surface energies through control of humidity

Bernardo Moreno Baqueiro Sansao [a,*], Jon J. Kellar [a,b], William M. Cross [a,b], Albert Romkes [c]

[a] Materials Engineering and Science Graduate Program, South Dakota School of Mines and Technology, United States
[b] Department of Materials and Metallurgical Engineering, South Dakota School of Mines and Technology, United States
[c] Department of Mechanical Engineering, South Dakota School of Mines and Technology, United States

ARTICLE INFO

Keywords:
Physical separation
Adhesion forces
Relative humidity
Sustainability

ABSTRACT

Many of the methods to classify and concentrate minerals and the subsequent extraction of metals takes place in water-based environments (aqueous solutions). Sustainable processing through the reduction of water consumption will become a key factor to make mining operations viable in the long term. In humid environments, capillary condensation of water can occur between the particle and substrate. The objective herein is to identify separation windows in which control of relative air humidity (RH) yields different substrate adhesion for hydrophilic and hydrophobic particles of different values of interfacial energy. Plasma cleaned glass beads, and trichloro(octadecyl)silane (TCOD) treated beads were poured on a plasma cleaned glass disk and an impact caused the detachment of particles. Impact tests performed under a range of RH showed that separation of plasma cleaned and TCOD treated particles can be achieved in 80% of the tests at humidity levels between 45% and 55%. The recovery of plasma cleaned particles was five times greater than TCOD treated particles at humidity levels between 50% and 55%.

1. Introduction

Many of the methods to classify and concentrate minerals and the subsequent extraction of metals take place in water-based environments (aqueous solutions). These processes include hydrocyclone classification, gravity-based concentration methods, froth flotation and leaching. In this regard, the consumption of water in the mineral industry can be on the order of 1.5 to 3.5 m^3 of water per metric ton of ore processed (Bleiwas, 2012). Compounding the use of water is the subsequent issues presented by storage of moisture-laden tailings in dams (Lyu et al., 2019). Thus, sustainable processing through the reduction of water consumption will become a key factor to make mining operations viable in the long term.

Froth flotation is the most common aqueous-based process to concentrate minerals with different surface properties. Specifically, particle wettability is the main property that influences the interaction between air bubbles and mineral surfaces. A hydrophobic mineral surface will adhere to air bubbles and be carried to the water/air interface, forming a mineralized froth. Minerals with hydrophilic surface character will not adhere to air bubbles. Thus, the governing mechanism for flotation is adhesion (or not) between the air bubble and the mineral particle. However, the flotation process requires tremendous amounts of water to achieve the desired concentrate grade.

The differences in adhesive forces between particles and a flat substrate have been investigated with the goal of development of a sustainable particle concentration system. Toward this end, many of the concepts associated with flotation mineral surface treatments have been utilized without the need for the continuous aqueous phase being present. Key to this investigation is a means to measure particle adhesive forces, and an understanding of the forces involved. In this regard, there are various techniques that have been applied to measure adhesive forces and the techniques used herein will be discussed subsequently (Zafar et al., 2014; Biresaw and Carriere, 2001; Madeira et al., 2018). When a dry particle is in contact with a dry surface, the primary adhesion forces involved are the van der Waals and electrostatic forces (Busnaina and Elsawy, 1998). According to Busnaina and Elsawy (Busnaina and Elsawy, 1998), the van der Waals forces can be heightened by increasing the contact area between particle and surface, i.e. causing deformation on either the particle or the substrate. This is not the case in this study since the particles and substrates used were rigid, and the

* Corresponding author at: South Dakota School of Mines and Technology, Department of Materials and Metallurgical Engineering, 501 East Saint Joseph Street, Rapid City, South Dakota, 57701, United States.
E-mail address: bernardo.sansao@mines.sdsmt.edu (B. Moreno Baqueiro Sansao).

https://doi.org/10.1016/j.mineng.2020.106680
Received 31 July 2020; Received in revised form 28 September 2020; Accepted 14 October 2020

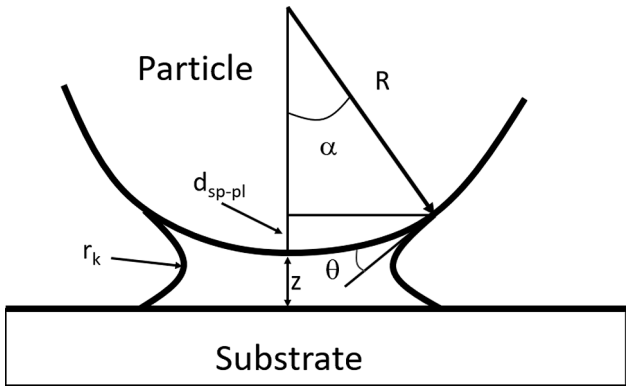

Fig. 1. Schematic diagram representing the capillary condensation of a sphere and a flat surface. R being the radius of the sphere and r_K the capillary radius, given by the Kelvin equation. (adapted from [8and10]).

deformation was neglected as it is expected to be small.

In humid environments, capillary condensation of liquids (in this case water) can occur between the particle and substrate. Fig. 1 shows an example of capillary condensation between a spherical particle and a flat surface with the assumption of contact angle of 0 degrees for both particle and substrate. The presence of capillary condensation engenders a capillary force, which is large compared to the van der Waals force and the electrostatic force as discussed by Busnaina (Busnaina and Elsawy, 1998). Thus, the relevant adhesive forces present in this particle/surface system are: van der Waals adhesion force (F_{vdW}), electrostatic image force (F_{cl}) and capillary force (F_c), represented by Equations 1 to 3, respectively. (Busnaina and Elsawy, 1998)

$$F_{vdw} = \frac{AR}{6z^2} \tag{1}$$

$$F_{cl} = \frac{Q}{6(D+z)^2} \tag{2}$$

$$F_c = 4\pi R\gamma_{LV} \tag{3}$$

Where A is the Hamaker constant, R is the radius of the spherical particle, z is the separation distance (taken as 4Å in the literature (Busnaina and Elsawy, 1998), Q is the charge carried by the particle, D is the particle diameter, and γ_{LV} is the surface tension of the condensed liquid (Busnaina and Elsawy, 1998). According to Feiler et al. (Feiler et al., 2005), to obtain the pull-off force related to the capillary force, F_c (Equation 3), it is necessary to consider the area where the Laplace pressure has influence. From the Kelvin equation, the Laplace pressure and the area have inverse dependence on the Kelvin radius (r_K). Therefore, Equation 3 is independent of relative air humidity. However, experiments in the literature (Feiler et al., 2005; Cleaver and Tyrrell, 2004) suggest that the adhesion increases as the humidity increases. Thus, Equation 3 is contradicted. This is likely because of assumptions made in the derivation of Equation 3 related to the vapor pressure used in the Kelvin equation. It is important to state that Fig. 1 is not represented by Equation 3, as the adhesion forces with the presence of capillary condensation involves the interfacial tension of the liquid and the contact length and the Laplace pressure and the contact area. A more relevant equation (Equation 4) to use in this case is the one proposed by Rabinovich et al. (Rabinovich et al., 2005) Where $d_{sp/pl}$ and α are as shown in Fig. 1.

$$F = \frac{4\pi R\cos\theta}{1 + z/d_{sp/pl}} \; 2\pi R\sin(\alpha)\sin(\theta+\alpha) \tag{4}$$

A review of the influence of relative humidity on particle adhesion by Cleaver and Tyrrell (Cleaver and Tyrrell, 2004) and other studies (McFarlane and Tabor, 1950) indicated that the roughness on the surface of the substrate and on the particle hinder the adsorption of water at the particle/substrate interface. Cleaver and Tyrrell (Cleaver and Tyrrell, 2004) concluded that increasing roughness decreased adhesion. The decrease in adhesion happens when the thickness of the film of water at the interface is on the same order of magnitude as of the asperity height (McFarlane and Tabor, 1950). In these cases, there are in fact many points of contact between the rough particle with the flat surface, or between the smooth particle and the rough surface, causing a decrease in adhesion. Also, the roughness of a surface could show a different capillary condensation of water over the asperities, causing a Wenzel state where the liquid completely penetrates into the asperities; or causing a Cassie-Baxter state where the air present in the asperities is trapped below the liquid drop (Erbil and Cansoy, 2009). We expect this aspect to be very important when crushed minerals are evaluated. For the experiments performed with glass beads that will be presented here, the roughness effect was neglected.

Experiments conducted using an atomic force microscope (AFM) with a glass sphere (R ≈ 10 μm) at the tip of the AFM cantilever on polished silicon wafers (roughness of 1–2 nm) showed a variation in adhesion between a glass sphere and a silicon wafer (Feiler et al., 2005). Specifically, a threshold in adhesion was observed around 60% relative air humidity (RH). Above this value, the adhesion force increased significantly. The pull-off force was approximated by Equation 3.

Similar behavior was achieved in experiments conducted on other systems (Busnaina and Elsawy, 1998). In one case, polystyrene latex (PSL) spheres (22 μm diameter) were deposited on polished silicon wafers. Here, the silicon wafer was rotated at 8,500 rpm for 120 s, generating detachment forces (drag force, lift force and centrifugal force). This procedure was repeated with humidity ranging from 10% to

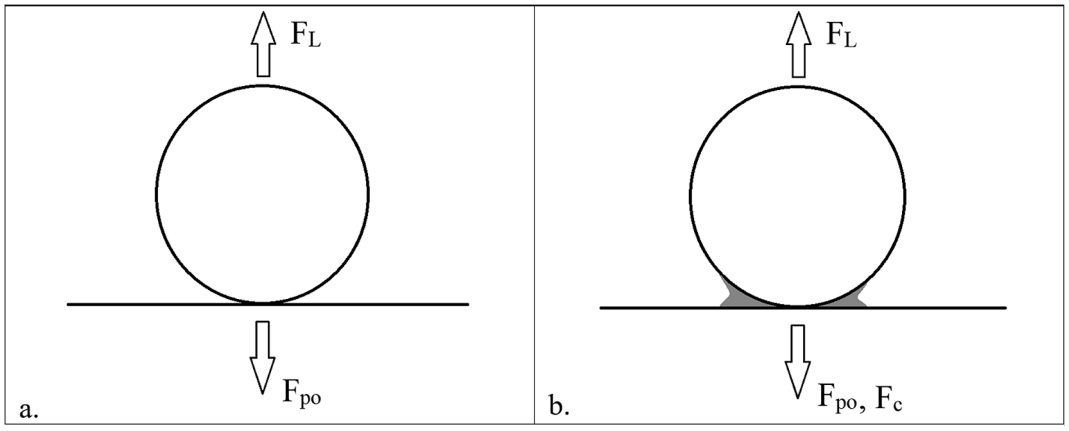

Fig. 2. Removal and adhesive forces involved in a. low relative humidity environment and in b. high relative humidity environment.

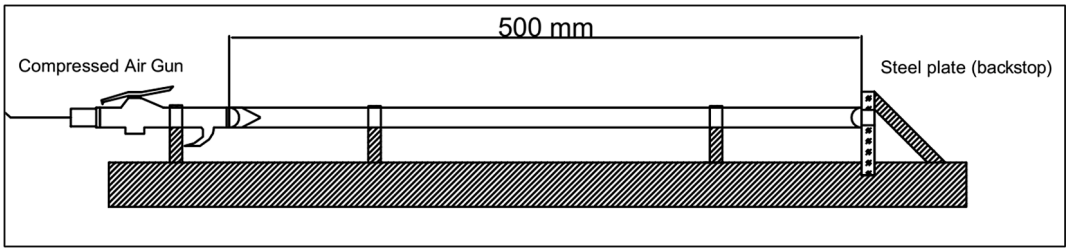

Fig. 3. Schematic of impact test apparatus.

90%.

In this case it was rationalized that at low relative humidity values the charge build-up is predominant, since PSL particles are insulators and silicon wafer is a semi-conductor (Busnaina and Elsawy, 1998). A gradual increase in RH from 45% to 80% and a steep increase from 80% to 85% were due to capillary condensation (increasing capillary force). In this example, the PSL is hydrophobic and the substrate is hydrophilic. The steep increase occurs at a greater relative humidity (80% versus 60%) than for the silica-based system (Busnaina and Elsawy, 1998), possibly because of the difference in hydrophobic character between the two systems.

For the case where spherical particles are sitting on a flat surface, a normal tensile force can cause separation if the lift-off force is greater than the adhesive forces. Fig. 2 shows the forces involved in low and high relative humidity environments.

Here F_{po} is the pull-off force given by the Johnson-Kendall-Roberts (JKR) model (Johnson et al., 1971), represented by Equation 5.

$$F_{po} = \frac{3}{4} W_a d \tag{5}$$

Where W_a is the thermodynamic work of adhesion and d is the particle diameter. The lift-off force required to remove the particle from the surface is then: $F_{po} + F_c$. Other methods (Zafar et al., 2014) to calculate the force necessary to remove the particles were used in the work presented here and will be discussed on the Materials and Methods Section.

Cleaver and Tyrrell (Cleaver and Tyrrell, 2004) reviewed many studies that investigated the influence of RH in particle adhesion. The measurement techniques used in the various studies included pendulum testing, deflection of fibers, centrifugal testing, use of electro-balances and AFM, with RH varying from 0% to 100%. Later studies, beyond those cited by Cleaver and Tyrrell, have been investigated (Feiler et al., 2005; Farshchi-Tabrizia et al., 2008). A table that encompasses prior research (McFarlane and Tabor, 1950; Zimon, 1982; Harnby et al., 1996; Berard et al., 2002; Jones et al., 2002; Rabinovich et al, 2002; Feiler et al., 2005; Farshchi-Tabrizia et al., 2008) including systems studied and findings is shown in Table S1, in the supplemental information. Only the parameters comparable to the work presented here are shown in Table S1. The first comparison was the size of the particles involved. In froth flotation a common size range is 10 μm and 150 μm – however, for completeness, studies with a top size of 1 mm were included in Table S1. The second relative comparison shown in Table S1 is the particle/substrate interaction. Finally, it should be noted that computer simulations were performed by Yang et al. (Yang et al., 2016) comparing other works (Farshchi-Tabrizia et al., 2008) also indicated the influence of RH in the particle adhesion.

With this background information, the objective of this paper is to identify separation windows in which control of relative air humidity yields different substrate adhesion for hydrophilic and hydrophobic particles of different values of interfacial energy. Zafar et al. (Zafar et al., 2014) used a mechanical approach to measure particle interfacial energies. In that research the RH in which the experiments were performed was reported (between 45% and 60% RH), but this parameter was not deliberately controlled. A similar mechanical approach was used herein, however relative humidity was controlled and varied for the

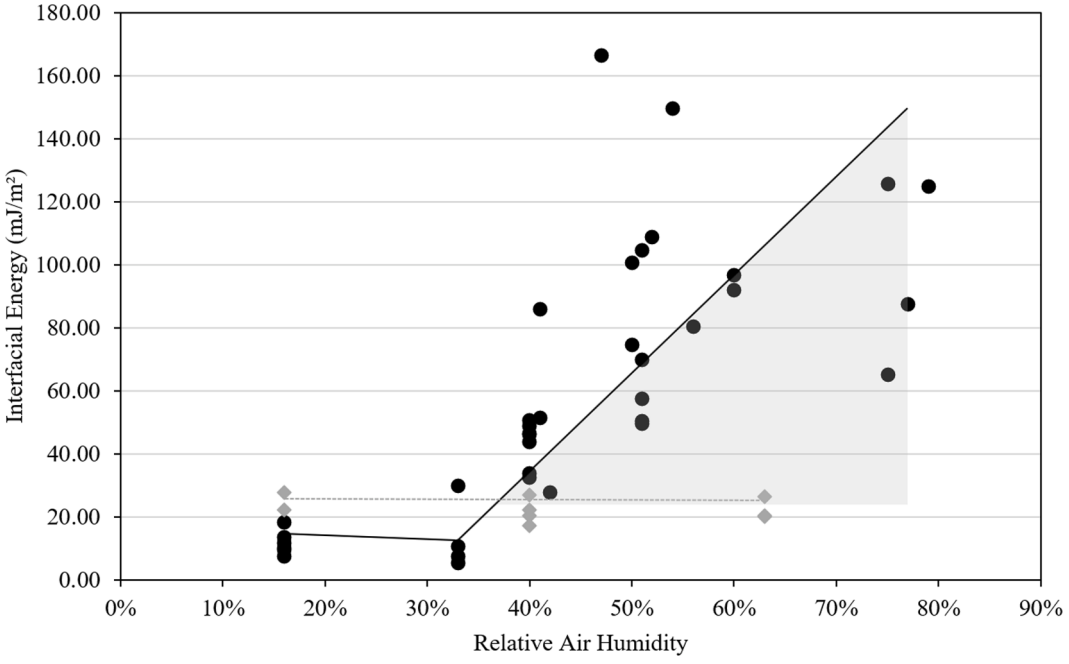

Fig. 4. Results of interfacial energy for different surface treatments at varying RH. A separation window can be explored due to differences in surface energy values at RH levels over 35% (gray region).

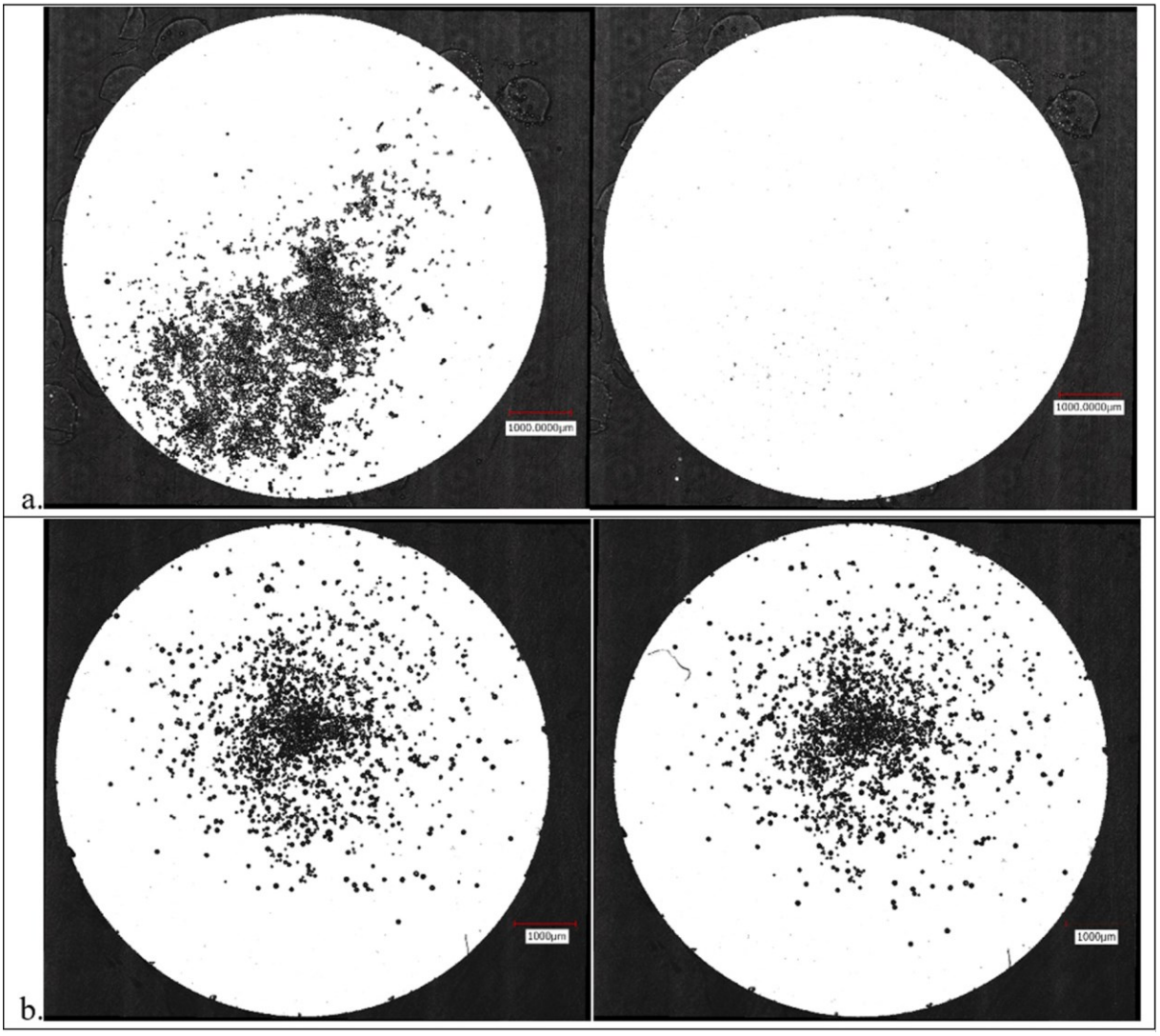

Fig. 5. Plasma cleaned beads on plasma cleaned disk before (left) and after (right) the impact at a) 16% RH and b) 75% RH. The capillary condensation enhances the adhesive forces holding more beads to the substrate.

measurement of particle separation. Ultimately the goal here is to determine whether particles with different surface properties (hydrophobic and hydrophilic), and hence different adhesive forces, can be separated as a function of RH.

2. Materials and methods

As mentioned earlier the interfacial energy was determined based on an impact test first developed by Zafar et al. (Zafar et al., 2014), and adapted for the needs of this research. A glass disk with the desired treatment was glued to an aluminum stub (25 mm long and 15 mm in diameter). A monolayer of glass spheres purchased from PolyScience (size range between 10 and 150 µm and density of 2.48 g/cm^3) was dispersed on the substrate. This size range was chosen because it is comparable to the size range of minerals often encountered in mineral beneficiation. Imaging of the disk and the beads was performed using an optical profilometer (Keyence VK 200) prior to the impact test. After initial imaging, the aluminum stub was propelled through a glass tube using an air compressor with a pressure regulator. The pressure was adjusted in order to achieve the desired velocity inside a horizontal tube with maximum length of 50 cm. An aluminum backstop with an opening of 12 mm was placed at the end of the glass tube. The stub accelerated and impacted on the backstop against the opening at the end of the tube. To record the velocity of impact and the duration of impact, a high-speed camera (IDT MotionProY Series 4) was used at 70,000 fps. Fig. 3 shows a schematic diagram of the testing equipment.

Equations (6) to (8) were used by Zafar et al. (Zafar et al., 2014), where F_{ad} is the JKR (Johnson et al., 1971) adhesive force, Γ is the interfacial energy and R is the particle radius of the largest particle left on the substrate to calculate the interfacial energy between two bodies. Equation (7) calculated the detachment force caused by a deacceleration of a given particle of mass *m*, where F_{det} is the detachment force, Δt is half of the time of impact (i.e. half of the time of contact between stub and backstop) and *v* is the impact velocity. The interfacial energy was then estimated from Equation (8), with $F_{det} = F_{ad}$.

$$F_{ad} = \frac{3}{2}\pi R\Gamma \tag{6}$$

$$F_{det} = \frac{m\Delta v}{\Delta t} \tag{7}$$

$$\Gamma = \frac{m\Delta v}{\Delta t \pi R}\frac{2}{3} \tag{8}$$

For the cases when the adhesive force is greater than the detachment

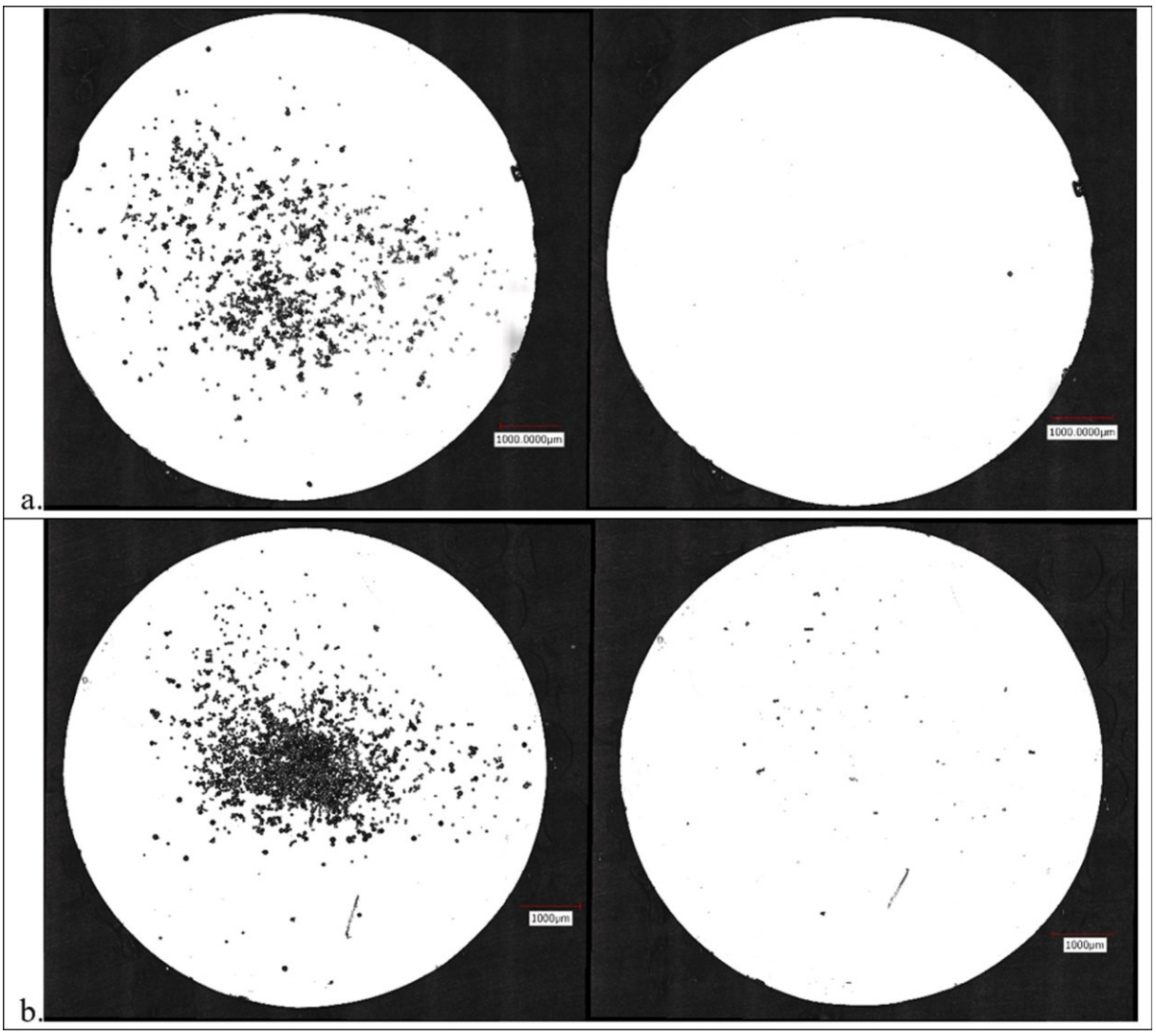

Fig. 6. TCOD treated beads on TCOD treated disk before (left) and after (right) the impact at a) 16% RH and b) 63% RH. The hydrophobic treatment is not susceptible to the capillary condensation.

force ($F_{ad} > F_{det}$), at a given particle size, the particles will not detach from the disk. When the adhesive force is equal to the detachment force, a critical particle size can be identified. The critical particle size is used in Equation 8 to calculate the interfacial energy. (Sansao et al., 2020)

Initial adhesion testing was conducted with no humidity control. It was found that the relative humidity fluctuated daily and the fluctuations were largely seasonal. For example, the average humidity measured inside the laboratory varied from 16% during the winter, to 55% during the summer. Measured relative air humidity levels are shown in Figure S1 in the supplemental information. Consequently, the testing apparatus (Fig. 3) was placed inside a transparent polycarbonate chamber to create a controlled humidity environment. Humidity was fed into the chamber using a humidifier (Homàsy Model HM161B) that was plugged in to a controller (Inkbird Humidity Controller IHC200) capable of measuring relative air humidity from 5% to 99%. To decrease the humidity inside the chamber a renewable silica-gel-based dehumidifier (Eva-Dry E-500) was used. The humidity controller was set to the desired level, the sensor then turned the humidifier on and turned it off as soon as the desired humidity was achieved. With the humidifier it is possible to increase the tested humidity above the summer maximum of 55% and exploit the interaction between surface treatments and water present in the air, in order to determine the effect of humidity on the ability to separate particles based upon adhesive forces.

To ensure that the particles and substrates would be conditioned to the set relative air humidity, the particles were sprinkled over the glass and left inside the chamber for at least 30 min prior to testing to allow all of the particles to contact the moisture in the air. The glass was glued on top of an aluminum stub and the test was performed as described earlier. For tests under controlled air humidity, two different glass treatments were used: plasma cleaned glass (hydrophilic and higher surface energy) and trichloro(octadecyl)silane (TCOD) (hydrophobic and lower surface energy). The purpose of using these two treatments was to compare the response of the interaction between hydrophilic surfaces, hydrophobic surfaces and a combination of hydrophobic particles and hydrophilic substrates.

The TCOD treatment was performed mixing 0.7 ml of TCOD and 20.0 ml of toluene for each gram of glass treated. The solution was then mixed for 2 h in a beaker. After the solution mixing, the glass specimens were dried at 150 degreesC for 2 h. To ensure that the hydrophobic treatment was effective, the contact angle between a drop of water and a glass disk was measured. For the glass beads, a fraction of beads was put in contact with water. The plasma cleaned glass beads would sink when in contact with water, and the TCOD treated beads would float/not mix with water.

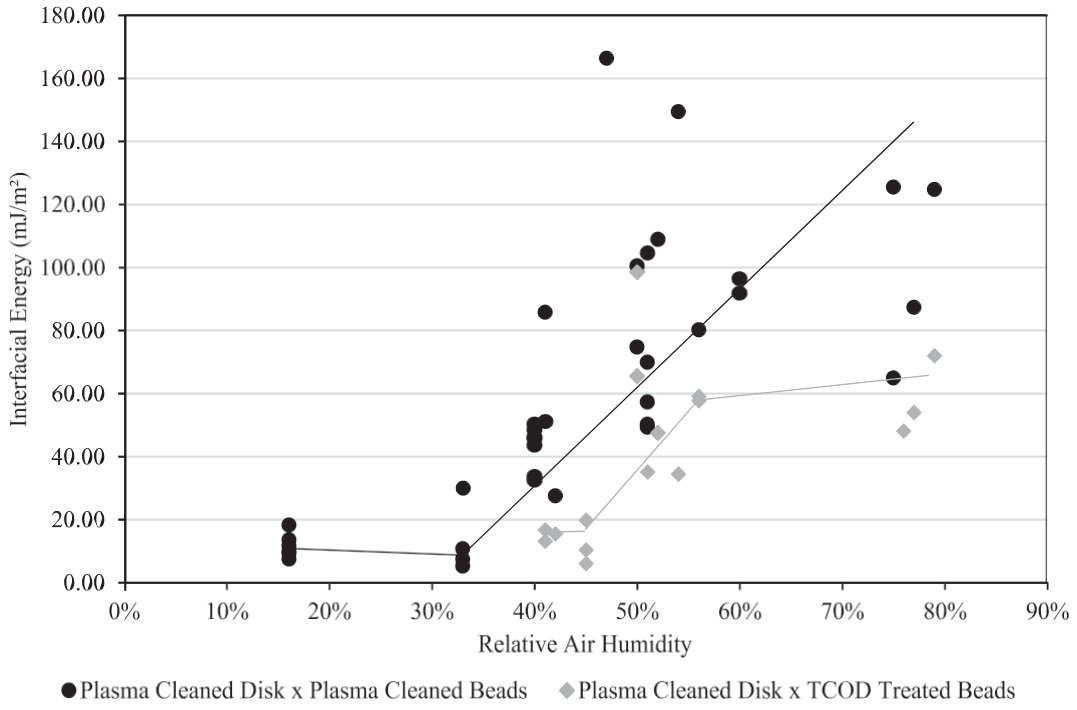

Fig. 7. Results of interfacial energy for different particle surface treatments on a plasma cleaned disk at varying RH.

Also, two different types of particles were placed on the same glass disk, in a way that it was possible to compare two treatment types under the same velocity of impact and duration of impact. Imaging of the beads on the disk was performed before and after the tests using the same profilometer mentioned in the previous section. The beads that remained attached to the disk after the impact were analyzed and the diameter was measured using ImageJ.

3. Results and discussion

For the plasma cleaned glass beads and plasma cleaned glass disks, the interfacial energy was calculated by applying Equation 8 and varying the RH from 16% to 79%. For the TCOD treated beads and TCOD treated disks, the interfacial energy was calculated for RH levels from 16% to 63%. The results of these tests are shown in Tables S3 and S4, respectively.

Fig. 4 graphically shows the results of the two surface treatments as a function of RH. It can be seen that the interfacial energy of plasma cleaned treated (hydrophilic and high surface energy) material is dependent of RH. Between 16% and 33% RH there is no significant change in the interfacial energy for the plasma cleaned (hydrophilic) particles. As the RH increases beyond 33%, the interfacial energy increases quite linearly from an average of 13.4 mJ/m^2 with a coefficient of variation of 0.84 to a value of 124.8 mJ/m^2 at 79% in a single measurement. Thus, it is possible to compare this behavior with the results from prior work (Busnaina and Elsawy, 1998; Busnaina and Elsawy, 1998), where at an RH threshold the capillary force will overcome the van der Waals force and hold the particles more strongly than the contact forces. In a subsequent investigation this effect was determined using an AFM where a maximum or continuous increase of adhesion force with increasing RH for hydrophilic surfaces was found (Farshchi-Tabrizia et al., 2008).

With respect to the TCOD treatment, with the RH varying from 16% to 63%, there is relatively little change associated with the interfacial energy of this surface treatment. The interfacial energy varied from 17.2 to 27.5 mJ/m^2. Literature values (Arkles, 2014) for this surface treatment indicate that TCOD coated surfaces should have a surface tension between 20 and 24 mJ/m^2.

Therefore, at RH values beyond ~ 35%, a separation window was explored by using the surface interaction of different surface treatments and properties to achieve a separation of particles. This first two analyses compare the same type of surface treatment for the substrate and particles. In order to evaluate the separation of particles with different surface properties in a single system, tests were performed using only plasma cleaned disks as substrate and having the two different types of beads treatment (plasma cleaned and TCOD) as particles.

To help demonstrate how RH impacts the adhesive forces, the difference for the hydrophilic and higher surface energy treatment for the hydrophobic and lower surface energy treatment are shown in Figs. 5 and 6. Fig. 5 shows a plasma cleaned disk with plasma cleaned beads before and after the impact at a) 16% RH and at b) 75% RH. Fig. 6 shows a TCOD treated disk with TCOD treated beads before and after the impact at a) 16% RH and at b) 63% RH. The visual before-and-after inspection clearly demonstrates the influence of RH on particle adhesion.

Nevertheless, for the TCOD treated material, capillary condensation may occur for the hydrophobic systems.

A third group of tests was performed, with plasma cleaned (hydrophilic) and TCOD particles (hydrophobic) sharing the same substrate, a plasma cleaned glass disk (hydrophilic). This 'mixed' system was chosen to help demonstrate the possibility of an actual mineral separation using a common substrate. Due to the limitations associated with the optical microscope used (featureless, same size, same color) surfaces, the particles were placed in different regions on the same disk. The results of interfacial energy at varying RH levels for plasma cleaned disk and TCOD treated particles are shown in Table S5.

Fig. 7 shows the results from Table S5 graphically. It is possible to observe that the interaction of hydrophobic particles and hydrophilic substrate (TCOD treated beads versus plasma cleaned disk) has changed when compared to particles and substrate of the same time (TCOD beads versus TCOD disks). However, and most importantly, there is still a difference of interfacial energy that can be exploited to reach separation of particles with different surface energies. As the plasma cleaned beads on a plasma cleaned surface interfacial energy continues to rise (results

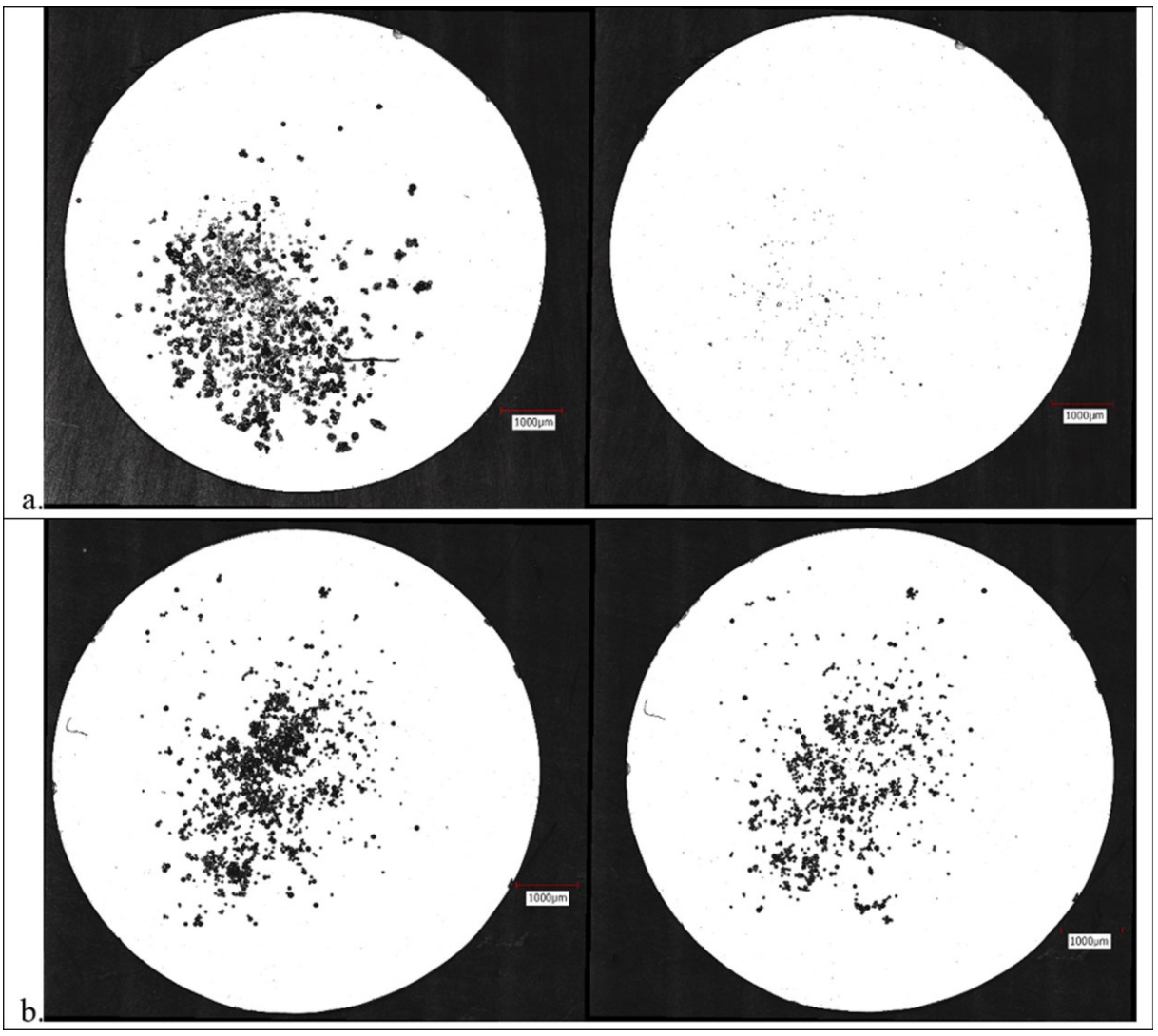

Fig. 8. TCOD treated beads on plasma cleaned disk before (left) and after (right) the impact at a) 50% RH and b) 75% RH. The hydrophilic property of the substrate does hold hydrophobic particles at high RH levels.

from Table S3), interfacial energy of TCOD treated beads increases less when RH varies from 55% to 79%.

Because the substrate is now hydrophilic and has higher surface energy, the hydrophobic particles have a different behavior at high RH levels, compared to the data shown in Fig. 4 (common particle/substrates). Fig. 7 shows that between 56% and 77% RH the increase in interfacial energy plateaus. The quantity of particles that remained attached after impact can be seen in Fig. 8, which shows a plasma cleaned disk with TCOD treated beads before and after the impact at a) 16% RH and at b) 75% RH.

From Fig. 7 it can be ascertained that the best separation would be between 55% and 75% RH. However, from Fig. 8, at 75% RH, a considerable amount of TCOD treated beads remained attached after the impact. Few TCOD treated beads were present after testing at 50% RH. Thus, a series of tests between 45% and 55% RH was performed to evaluate the separation and recovery of particles with different surface treatment on the same substrate. Plasma cleaned beads were poured on the upper region and TCOD treated beads were poured on the lower region of the same substrate. Fig. 9 shows the results of tests at a) 37% RH and b) 52% RH.

As expected, as the RH increases, the adhesion of hydrophobic particles on the hydrophilic substrate increases. Using ImageJ, it was possible to measure the area covered by the particles before and after the impact with the objective to estimate the recovery of particles retained. The recovery was calculated as follows:

$$Recovery = \frac{Area\ occupied\ by\ the\ beads\ after\ impact}{Area\ occupied\ by\ the\ beads\ before\ impact} \quad (8)$$

The goal here was to have a good recovery of plasma cleaned particles (considerable quantity of beads remaining attached after the impact) and a low recovery of TCOD treated particles (few low-surface-energy particles remaining). Fig. 10 shows the results of the tests from 37% to 54% of RH.

Examination of Fig. 10 shows that the recovery of plasma cleaned particles is relatively small when the RH is between 37 and 45%. However, when the RH is between 45 and 54% the recovery increases. For the tests between 47% and 54% the recovery of plasma cleaned particles was, on average, five times greater than the recovery of TCOD treated particles. These results indicate that a method of separation can be exploited in controlled relative air humidity environments for particles with different adhesive properties.

A next step for this research is to apply the same method to evaluate the separation of mineral particles with different surface properties; as well as to develop more sustainable methods to modify particle surfaces

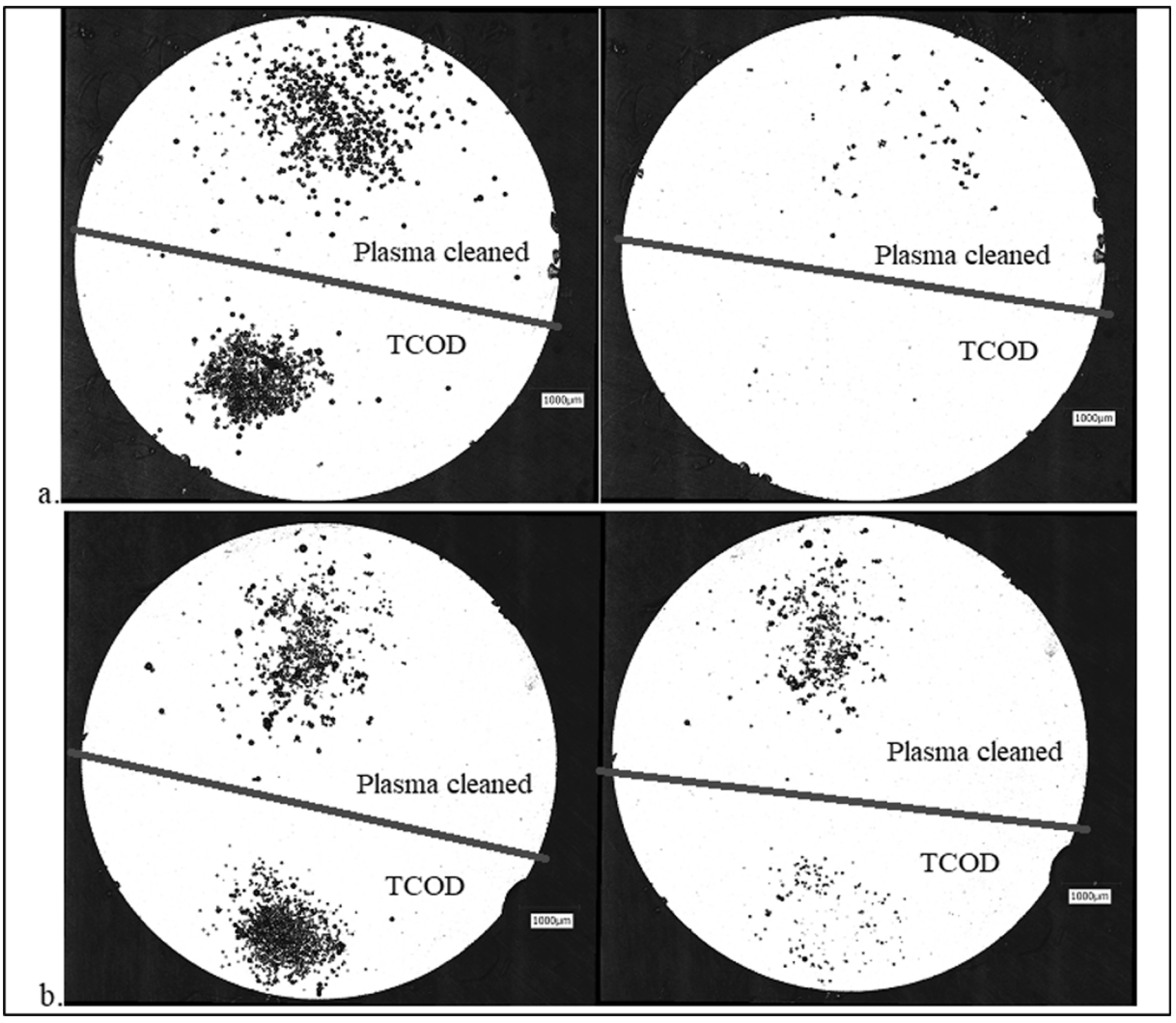

Fig. 9. TCOD treated beads and plasma cleaned beads on plasma cleaned disk before (left) and after (right) the impact at a) 37% RH and b) 52% RH.

in order to achieve separation for a given ore. This way, the consumption of water can be addressed, since the water consumed to control RH in a room is smaller than the consumption of water by flotation process. In addition, the effect of surface roughness of these mineral particles will be evaluated.

4. Conclusions

An impact test apparatus was used to determine the interfacial energies of a model system with varying relative air humidity. The behavior of the interfacial energy with varying RH is comparable to other methods used. It was observed that capillary condensation did increase the adhesive forces of hydrophilic materials. A separation window was identified and the differences in interfacial energy for a hydrophilic surface and for a hydrophobic surface can be exploited in order to achieve the separation of particles.

When in contact with a hydrophilic substrate, hydrophobic particles can be attached more strongly due to capillary condensation with higher-surface-energy substrates. In the cases where two different types of particles were under the same test conditions, plasma cleaned particles showed a higher recovery in 80% of the tests when the RH varied from 37% to 54%. And the recovery of the plasma cleaned particles proved to be five times greater, on average, when compared to the TCOD treated particles for RH between 47% and 54%. These measurements will be used toward development of a sustainable system that uses little water to separate and concentrate fine minerals. This data will be coupled with computer simulations in order to predict ideal conditions to achieve mineral separation. Also, a lab scale separator will be designed to determine the efficacy of mineral separations based upon adhesive forces with controlled relative humidity.

CRediT authorship contribution statement

Bernardo Moreno Baqueiro Sansao: Conceptualization, Methodology, Validation, Formal analysis, Investigation, Data curation, Writing - original draft, Writing - review & editing. **Jon J. Kellar:** Supervision, Funding acquisition, Conceptualization, Validation, Investigation, Resources, Project administration, Data curation, Writing - original draft, Writing - review & editing, Visualization. **William M. Cross:** Supervision, Funding acquisition, Conceptualization, Validation, Investigation, Resources, Project administration, Data curation, Writing - original draft, Writing - review & editing, Visualization. **Albert Romkes:** Supervision, Funding acquisition, Conceptualization, Project administration, Writing - review & editing.

Declaration of Competing Interest

The authors declare that they have no known competing financial

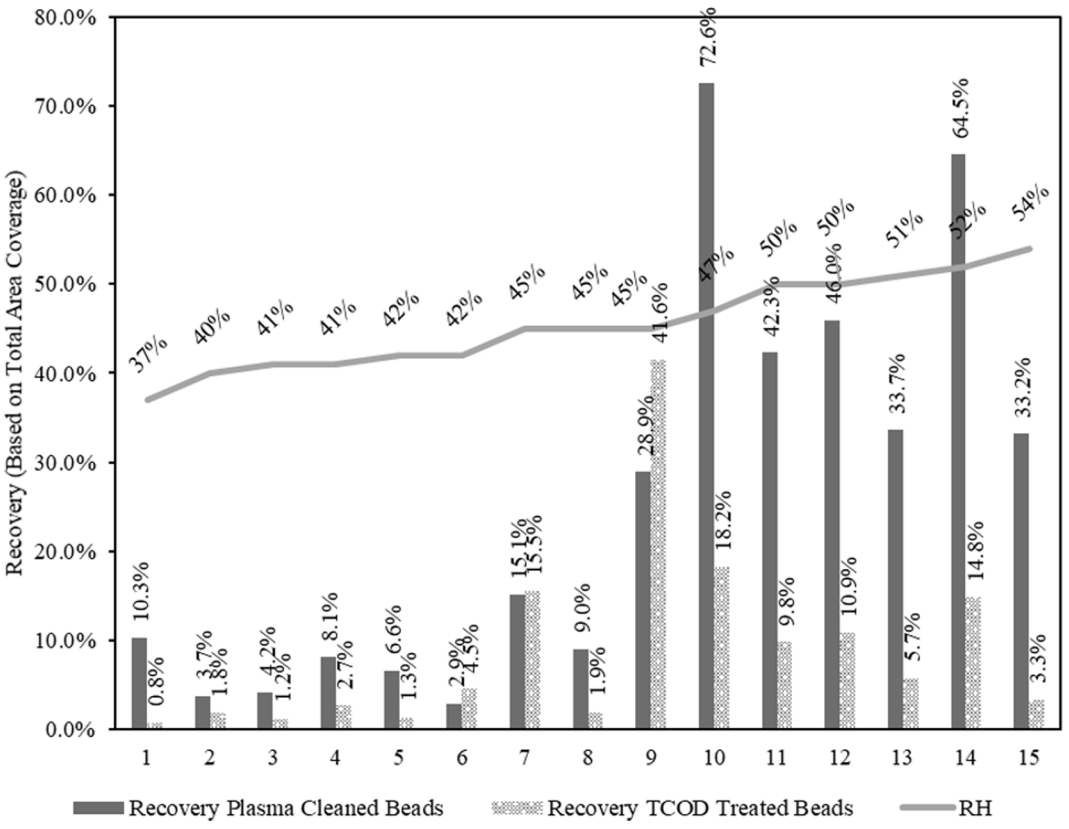

Fig. 10. Recovery of particles with varying RH.

interests or personal relationships that could have appeared to influence the work reported in this paper.

Acknowledgements

Support of the research is through the National Science Foundation Grant (NSF) #1805550 Sustainable System for Mineral Beneficiation. Also, thank you to Dr. Umair Zafar for his helpful discussion as well as Ms. Kathryn Bozer and Mr. Bobby Santore (NSF Grants #1460912 and #1757799 (REU Site: Back to the Future)) for their generation of preliminary data.

Appendix A. Supplementary data

Supplementary data to this article can be found online at https://doi.org/10.1016/j.mineng.2020.106680.

References

Bleiwas, Donald I. (2012). Estimated water requirements for the conventional flotation of ores. USGS pages 2-3.

Lyu, Z., Chai, J., Xu, Z., Qin, Y., Cao, J., 2019. A Comprehensive Review on Reasons for Tailings Dam Failures Based on Case History. Advances in Civil Engineering 2019, 1–18.

Zafar, U., Hare, C., Hassanpour, A., Ghadiri, M., 2014. Drop test: A new method to measure the particle adhesion force. Powder Technology 264, 236–241.

Biresaw, G., Carriere, C.J., 2001. Correlation between mechanical adhesion and interfacial properties of starch/biodegradable polyester blends. J. Polym. Sci. B Polym. Phys. 39 (9), 920–930.

Madeira, D. M. F., Vieira, O., Pinheiro L. A., & Carvalho, B. d. M. (2018). Correlation between surface energy and adhesion force of polyethylene/paperboard: a predictive tool for quality control in laminated packaging. Hindawi International Journal of Chemical Engineering, 2018, Article ID 2709037, 7 pages, https://doi.org/10.1155/2018/2709037.

Busnaina, A. A., Elsawy, T. (1998). The Effect of Relative Humidity on Particle Adhesion and Removal. Proceedings of the 21st Annual Meeting of the Adhesion Society, 1998. Georgia, USA. pages 315-317.

Busnaina, A. A., Elsawy, T. (1998). The Measurement of Particle Adhesion Forces in Humid and Dry Environments. Proceedings of the 21st Annual Meeting of the Adhesion Society, 1998. Georgia, USA. pages 394-397.

Feiler, A.A., Jenkins, P., Rutland, M.W., 2005. Effect of relative humidity on adhesion and frictional properties of micro- and nano-scopic contacts. Journal of Adhesion Science and Technology 19 (3-5), 165–179.

Cleaver, J.A.S., Tyrrell, J.W.G., 2004. The Influence of Relative Humidity on Particle Adhesion – a Review of Previous Work and the Anomalous Behaviour of Soda-lime Glass. KONA 22 (0), 9–22.

Rabinovich, Y. I., Esayanur, M. S., and Moudgil, B. M. (2005). Capillary Forces between Two Spheres with a Fixed Volume Liquid Bridge: Theory and Experiment. Langmuir, 21, PAGES 10992-10997.

McFarlane, J.S., Tabor, D., 1950. Adhesion of solids and the effect of surface films. Proceedings of the Royal Society A 202, 224–243.

Erbil, H.Y., Cansoy, C.E., 2009. Range of Applicability of the Wenzel and Cassie Baxter Equations for Superhydrophobic Surfaces †. Langmuir 25 (24), 14135–14145.

Johnson, K.L., Kendall, K., Roberts, A.D., 1971. Surface energy and the contact of elastic solids. Proceedings of the Royal Society A 324, 301–313.

Farshchi-Tabrizia, M., Kappl, M., Butt, H.-J., 2008. Influence of Humidity on Adhesion: An Atomic Force Microscope Study. Journal of Adhesion Science and Technology 22 (2), 181–203.

Zimon, A.D. (Ed.), 1982. Adhesion of Dust and Powder. Springer US, Boston, MA.

Harnby, N., Hawkins, A. E., Opalinski, I. (1996). Measurement of the adhesional force between individual particles with moisture present Part 2: A Novel Measurement Technique. Chemical Engineering Research and Design, 74 A, pages 616-626.

Berard, V., Lesniewska, E., Andres, C., Pertuy, D., Laroche, C., Pourcelot, Y., 2002. Dry powder inhalers: influence of humidity on topology and adhesion studied by AFM. International Journal of Pharmaceutics 232, 213–224.

Jones, R., Pollock, H.M., Cleaver, J.A.S., Hodges, C., 2002. Adhesion forces between glass and silicon surfaces in air studied by AFM: Effects of relative humidity, particle size, roughness, and surface treatment. Langmuir 18, 8045–8055.

Rabinovich, Y.I., Adler, J.J., Esayanur, M.S., Ata, A., Singh, R.K., Moudgil, B.M., 2002. Capillary forces between surfaces with nanoscale roughness. Advances in Colloid and Interface Science 96 (1-3), 213–230.

Yang, L.i., Hu, JunHui, Bai, K., 2016. Capillary and van der Waals force between microparticles with different sizes in humid air. Journal of Adhesion Science and Technology 30 (5), 566–578.

Sansao, B. M. B., Kellar, J. J., Cross, W. C., Schottler, K., Romkes, A. (2020) Comparison of surface energy and adhesion energy of surface-treated particles. Paper under review, submitted to Powder Technology.

Arkles, B., et al., 2014. Silane Coupling Agents: Connecting Across Boundaries. Gelest, Inc., Version 3, pg 5.